
Article:
Gibson, R.R., Cornel, E.J., Musa, O.M. et al. (2 more authors) (2020) RAFT dispersion polymerisation of lauryl methacrylate in ethanol–water binary mixtures: synthesis of diblock copolymer vesicles with deformable membranes. Polymer Chemistry, 11 (10). pp. 1785-1796. ISSN 1759-9954

https://doi.org/10.1039/c9py01768b

RAFT dispersion polymerisation of lauryl methacrylate in ethanol-water binary mixtures: synthesis of diblock copolymer vesicles with deformable membranes

Received 00th January 20xx,
Accepted 00th January 20xx

DOI: 10.1039/x0xx00000x

R. R. Gibson[a], E. J. Cornel[a], O. M. Musa[b], A. Fernyhough[c] and S. P. Armes[a]*

Polymerisation-induced self-assembly (PISA) is widely recognised to be a powerful platform technology for the rational synthesis of diblock copolymer nano-objects. RAFT alcoholic dispersion polymerisation is an important PISA formulation that has been used to prepare block copolymer spheres, worms and vesicles. In this study, we have utilised the RAFT dispersion polymerisation of lauryl methacrylate (LMA) using a poly(*N*-(2-methacryloyloxy)ethyl pyrrolidone) (PNMEP) stabiliser in order to prepare vesicles with highly deformable membranes. More specifically, a $PNMEP_{28}$ macro-CTA was chain-extended with LMA in an 80:20 w/w ethanol-water mixture to produce a series of $PNMEP_{28}$-$PLMA_x$ diblock copolymer nano-objects ($M_w/M_n \leq 1.40$; LMA conversions ≥ 99% in all cases, as indicated by ^{1}H NMR spectroscopy). Differential scanning calorimetry studies confirmed that the membrane-forming PLMA block had a relatively low glass transition temperature. Transmission electron microscopy and small angle X-ray scattering were used to identify copolymer morphologies for these highly asymmetric diblock copolymers. A mixed sphere and vesicle morphology was observed when targeting x = 43, while polydisperse vesicles were obtained for x = 65-151. Slightly smaller vesicles with lower mean aggregation numbers and thicker membranes were obtained when targeting higher PLMA DPs. A minor population of sheet-like lamellae was observed for each target copolymer composition, with lamellar stacking leading to a structure peak in the scattering patterns recorded for $PNMEP_{28}$-$PLMA_{129}$ and $PNMEP_{28}$-$PLMA_{151}$. Bearing in mind potential industrial applications, RAFT chain-end removal strategies were briefly explored for such $PNMEP_{28}$-$PLMA_x$ vesicles. Thus, 96% of dithiobenzoate chain-ends could be removed within 3 h at 50 °C via LED irradiation of a 7.5% aqueous dispersion of $PNMEP_{28}$-$PLMA_{87}$ vesicles at a wavelength of 405 nm. This appears to be an attractive method for RAFT chain-end removal from diblock copolymer nano-objects, particularly those comprising highly hydrophobic cores.

* Author to whom correspondence should be addressed (s.p.armes@sheffield.ac.uk)

Introduction

Poly(*N*-vinylpyrrolidone) (PNVP) is highly biocompatible and hence widely used in the health and personal care industry.[1] [2,3] For example, it is employed as an excipient/binder in various drug formulations.[4] Its excellent film-forming properties are utilised for hair sprays[3] and it also acts as a lubricant for contact lenses and eye drops when copolymerised with silicones.[5] Unfortunately, only a limited number of monomers such as acrylics and vinyl acetate[6–9] can be copolymerised readily with NVP via free radical polymerisation. On the other hand, a methacrylic analogue, *N*-(2-methacryloyloxy)ethyl pyrrolidone (NMEP), copolymerises well with many methacrylic monomers.[10–14] Recently, the Armes group have evaluated PNMEP as a replacement for PNVP for the synthesis of well-defined pyrrolidone-functional block co-polymers.[13–15]

Cunningham *et al.* reported using PNMEP as a steric stabiliser for the synthesis of diblock copolymer nano-objects via reversible addition-fragmentation chain transfer (RAFT) alcoholic dispersion polymerisation of BzMA,[12] , which is an example of polymerisation-induced self-assembly (PISA).[16–20] Well-defined spheres, worms or vesicles could be obtained depending on the relative volume fraction of the PNMEP and PBzMA blocks. However, relatively long reaction times (24 h) were required for high BzMA conversions. This problem is well documented for various RAFT alcoholic dispersion formulations.[21–30] In this context, Zhang *et al.* reported the effect of adding water to the RAFT alcoholic dispersion polymerisation of benzyl methacrylate on the final copolymer morphology.[21] Using just 5 % water as a co-solvent enabled either spheres, worms or vesicles to be obtained when increasing the target degree of polymerisation (DP) of the core-forming PBzMA block. Similarly, Jones and co-workers reported that addition of increasing amounts of water to an alcoholic RAFT PISA formulation significantly increased the rate of polymerisation but limited the copolymer morphology to kinetically-trapped spheres.[25] The faster kinetics was attributed to a higher local monomer concentration caused by stronger partitioning of the BzMA monomer inside the growing nascent nanoparticles.

Lauryl methacrylate (LMA) is a commercially important hydrophobic monomer; PLMA-based copolymers have been used as viscosity modifiers in engine oil formulations.[31] Its relatively low glass transition temperature (T_g), -65 °C,[32] affords excellent film-forming properties, which are utilised in the cosmetics industry for both hair conditioning[33] and also to produce water-resistant barriers for skin care products.[34] Dong and co-workers reported the synthesis of PLMA-PNMEP diblock copolymers via RAFT *solution* polymerisation conducted in chloroform.[11,35,36] Unfortunately, only relatively low monomer

[a] Dainton Building, Department of Chemistry, University of Sheffield, Brook Hill, Sheffield, South Yorkshire, S3 7HF, UK.
[b] Ashland Inc., 1005 US 202/206, Bridgewater, New Jersey 08807, USA.
[c] Ashland Inc., Listers Mills, Heaton Rd, Bradford, West Yorkshire, BD9 4SH, UK.

† Footnotes relating to the title and/or authors should appear here.
Electronic Supplementary Information (ESI) available: [details of any supplementary information available should be included here]. See DOI: 10.1039/x0xx00000x

conversions (typically < 86%) could be achieved within 24 h at 60 °C, regardless of the target copolymer composition. However, chloroform gel permeation chromatography (GPC) studies confirmed that low-dispersity diblock copolymers were obtained (M_w/M_n < 1.21). Subsequently, these diblock copolymers were self-assembled in THF[11] or *n*-dodecane[35,36] to produce dilute dispersions of various types of nano-objects via traditional post-polymerisation processing.

Recently, Lowe and co-workers reported the PISA synthesis of well-defined spheres, worms or vesicles comprising low T_g core-forming blocks.[37] More specifically, RAFT dispersion polymerisation of 3-phenylpropyl methacrylate in ethanol was conducted using a poly(2-(dimethylamino)ethyl methacrylate) (PDMA) steric stabiliser block. Interestingly, a reversible worm-to-sphere transition with concomitant degelation was observed on heating up to 70 °C. This was attributed in part to the relatively low T_g of the core-forming poly(3-phenylpropyl methacrylate) block, which was determined to be approximately 2 °C by differential scanning calorimetry (DSC) measurements.

Herein we report the highly convenient PISA synthesis of LMA-rich PNMEP-PLMA diblock copolymer vesicles in ethanol-water mixtures. Bearing in mind potential industrial applications, RAFT chain-end removal strategies have been briefly explored for such diblock copolymer nanoparticles.

Experimental

Materials

N-(2-(Methacryloyloxy)ethyl pyrrolidone (NMEP; 98% purity) was kindly provided by Ashland Inc. (Delaware, USA) and was used without further purification. Lauryl methacrylate (LMA), ethanol (≥99.8%), 2-cyano-2-propyl benzodithioate (CPDB) and d_1-chloroform were purchased from Sigma Aldrich UK. 4,4'-Azobis(4-cyanovaleric acid) (ACVA; 99%) was purchased from Alfa Aesar (Heysham, UK). d_6-Acetone and d_4-methanol was purchased from Goss Scientific Instruments Ltd. (Cheshire, UK). Deionised water was used for all experiments.

Synthesis of $PNMEP_{28}$ macro-CTA by RAFT solution polymerisation in ethanol

The protocol for the preparation of $PNMEP_{28}$ macro-CTA is described below. NMEP (9.37 g, 47.4 mmol), CPDB RAFT agent (0.30 g, 1.36 mmol; target DP = 35), ACVA (76.0 mg, 0.27 mmol; CPDB/ACVA molar ratio = 5.0) and ethanol (14.59 g, 40% w/w solids) were weighed into a 50 mL round-bottom flask immersed in an ice bath and degassed with continuous stirring for 30 min. The reaction was allowed to proceed for 270 min in an oil bath set to 70 °C, resulting in a monomer conversion of 90% as judged by ^{1}H NMR spectroscopy. The polymerisation was then quenched by exposing the hot reaction solution to air and cooling to 20 °C. The crude polymer was precipitated into excess diethyl ether to remove residual monomer before freeze-drying from water to afford a dry pink powder. The mean DP was calculated to be 28 by comparing the integrated aromatic protons arising from the dithiobenzoate RAFT end-groups at 7-8 ppm to the methylene carbonyl proton signal at 2.5 ppm. GPC analysis using chloroform eluent indicated an M_n of 5 000 g mol^{-1} and an M_w/M_n of 1.23 against a series of ten near-monodisperse poly(methyl methacrylate) calibration standards.

Polymerisation-induced self-assembly synthesis of $PNMEP_{28}$-$PLMA_x$ diblock copolymer nanoparticles via RAFT dispersion polymerisation of LMA in an ethanol/water mixture at 70 °C

A typical protocol for the synthesis of $PNMEP_{28}$-$PLMA_{87}$ (LMA/NMEP mass ratio = 4:1) is described as follows: $PNMEP_{28}$ macro-CTA (0.15 g, 26.10 µmol), LMA (0.58 g, 2.27 mmol; target DP = 87 and ACVA (1.50 mg, 5.22 µmol; 0.19 mL of a 7.89 g dm^{-3} ethanolic stock solution; $PNMEP_{28}$/ACVA molar ratio = 5.0) were dissolved in an 80:20 w/w ethanol-water mixture (2.92 g). The reaction vial was sealed and degassed under N_2 for 30 min before placing in a pre-heated oil bath set at 70 °C for 16 h. The polymerisation was quenched by exposing the hot reaction solution to air and cooling to 20 °C. The resulting diblock copolymer nanoparticles were characterised by ^{1}H NMR spectroscopy, DLS and TEM with 0.1% w/w dispersions being prepared via dilution using an 80:20 w/w ethanol-water mixture. Chloroform GPC analysis indicated an M_n of 19 800 g mol^{-1} and an M_w/M_n of 1.28. Other diblock compositions were prepared by adjusting the amount of LMA monomer to target LMA/NMEP mass ratios ranging between 2:1 and 7:1. For these additional syntheses, the volume of the continuous phase was adjusted to maintain an overall solids concentration of 20% w/w (see Table 1 for the corresponding DPs of the PLMA blocks). ^{1}H NMR analysis indicated that more than 98% monomer conversion was achieved in all cases.

Protocol for cleavage of RAFT end-groups from $PNMEP_{28}$-$PLMA_{87}$ diblock copolymer nanoparticles using blue LED light irradiation.

The dithiobenzoate end-groups within $PNMEP_{28}$-$PLMA_{87}$ vesicles were cleaved according to the following protocol. A 20% w/w copolymer dispersion (1.0 g) was diluted to 7.5% w/w using deionised water (1.7 g). This dispersion was then placed in a water-jacketed Schlenk tube wrapped in blue LED light strips (λ = 405 nm, 0.37 mW cm^{-2}; see Figure S9 in the ESI) with the temperature of the recirculating water set to 50 °C. Aliquots of this reaction mixture were taken periodically and analysed using UV GPC (detector set at λ = 308 nm).

Copolymer characterisation

^{1}H NMR spectroscopy. d_4-Methanol was used to record ^{1}H NMR spectra of the $PNMEP_{28}$ macro-CTA and d_1-chloroform and d_6-acetone were used to analyse the $PNMEP_{28}$-$PLMA_x$ diblock copolymers in a 10:1 mass ratio. Spectra were recorded using a 400 MHz Bruker Avance 400 spectrometer with 64 scans being averaged per spectrum.

Gel permeation chromatography (GPC). Molecular weight data for both the PNMEP homopolymer precursor and the series of $PNMEP_{28}$-$PLMA_x$ diblock copolymers were obtained using

chloroform GPC at 35 °C, with the eluent containing 0.25% TEA by volume. Two Polymer Laboratories PL gel 5 µm Mixed C columns were connected in series to a Varian 390 multidetector suite (refractive index detector) and a Varian 290 LC pump injection module using a 1.0 mL min^{-1} flow rate. Ten near-monodisperse poly(methyl methacrylate) standards (PMMA; M_n = 625 – 618 000 g mol^{-1}) were used for calibration and data were analysed using Varian Cirrus GPC software. UV GPC chromatograms were obtained simultaneously by detection at a fixed wavelength of 308 nm, which corresponds to the absorption maximum of the dithiobenzoate RAFT end-groups.

Dynamic light scattering (DLS). A Malvern Zetasizer NanoZS instrument was used to determine the intensity-average hydrodynamic diameter of the copolymer nanoparticles at 20 °C at a scattering angle of 173°. As-synthesised dispersions were diluted to 0.1% w/w using either an 80:20 w/w ethanol-water mixture, deionised water or pure ethanol and analysed using disposable 1.0 cm path length plastic cuvettes. Data were averaged over three consecutive measurements (with 10 sub-runs per run) for each sample. Sphere-equivalent intensity-average diameters were calculated for diblock copolymer nano-objects via the Stokes–Einstein equation, which assumes perfectly monodisperse, non-interacting spheres. Aqueous electrophoresis measurements were also conducted at 20 °C using the same instrument for 0.1% w/w nanoparticle dispersions prepared using 1 mM KCl as the diluent. The solution pH was adjusted using either HCl or KOH as required. Zeta potentials were calculated from the Henry equation using the Smoluchowski approximation.

Transmission electron microscopy (TEM). Copper/palladium grids were surface-coated in-house to produce a thin film of amorphous carbon before being plasma glow-discharged for 40 s producing a hydrophilic surface. A single droplet (15 µL) of a 0.1% w/w copolymer dispersion (prepared by serial dilution using an 80:20 w/w ethanol-water mixture) was placed on a grid for 60 s, blotted to remove the excess solution and then stained using an aqueous uranyl formate solution (0.75% w/v) for 20 s. Excess negative stain was removed by careful blotting and the grid was then dried using a vacuum hose. A FEI Tecnai Spirit microscope operating at 80 kV equipped with a Gatan 1kMS600CW CCD camera was used to image the grids.

Small-angle X-ray scattering (SAXS). SAXS patterns were recorded at a national synchrotron facility (station I22, Diamond Light Source, Didcot, Oxfordshire, UK) using monochromatic X-ray radiation (λ = 0.124 nm with q ranging from 0.01 to 2.00 nm-1 where $q = 4\pi\sin\Theta/\lambda$ is the length of the scattering vector and Θ is one-half of the scattering angle) and a 2D Pilatus 2M pixel detector (Dectris, Switzerland). A glass capillary of 2 mm diameter was used as a sample holder and all measurements were conducted on 1.0% w/w copolymer dispersions in 80:20 w/w ethanol-water mixtures. X-ray scattering data were reduced and normalised using standard routines by the beamline and were further analysed using Irena SAS macros for Igor Pro.

Reverse phase high performance liquid chromatography (Reverse phase HPLC). HPLC analysis was performed on an HP 1100 series LC equipped with a quadratic pump, an autosampler and a diode array detector. An Agilent Poroshell EC-C18 100 x 4.6 mm column with a particle size of 3.5 µm was used at 40 °C. The mobile phase consisted of water with 0.1 % (v/v) orthophosphoric acid and acetonitrile run under gradient conditions (acetonitrile varied from 5% to 100 % in 20 min with a 2-min hold at 100 % before re-equilibriation at 5 % for 5 min) at a flow rate of 0.40 mL min^{-1}, a run time of 27 min and an injection volume of 5 µL. The analyte was detected at a wavelength of 210 nm normalised against a 360 nm reference wavelength. Nanoparticle dispersions were diluted to 2.0% w/w using deionised water. The resulting dispersions were shaken for 20 min and decanted into centrifugal cut-off filters (Merck Amicon Ultra-4, 3 KDa nominal molecular weight) to remove high molecular weight material. These were centrifuged at an RCF of 8422 g (9000 rpm; rotor radius = 9.3 cm) for 20 min to produce approximately 4 ml of aqueous filtrate for evaluation of residual NMEP monomer. Concentration was measured based on the detector response to external NMEP standards of known concentration.

Gas chromatography (GC). GC analysis for residual LMA was conducted using an Agilent 7890A series GC equipped with a Restek Rxi-624Sil-MS capillary column (30 m x 0.32 mm, D= 1.8 µm), hydrogen carrier gas and a flame ionisation detector (FID). Carrier gas velocity was fixed at 45.5 cm s^{-1}. Injection volume was fixed at 2 µl. LMA content of reaction mixtures was calculated against the detector response towards a series of LMA external standards of known concentration (5 - 100 µg ml^{-1}). The inlet temperature was fixed at 225 °C and the initial oven temperature was 100 °C. The oven programme was a 2 min isothermal hold followed by a 10 °C min^{-1} ramp to 300 °C and a 4 min hold. The detector temperature was maintained at 300 °C. Samples were extracted using acetone (0.2 g in 2 ml) and filtered through a 0.45 µm PTFE filter prior to injection.

Differential Scanning Calorimetry (DSC). Glass transition temperatures (T_gs) for six $PNMEP_{28}$-$PLMA_x$ diblock copolymers were determined using a Perkin-Elmer Pyris 1 differential scanning calorimeter from −90 to 100 °C at a heating/cooling rate of 10 °C min^{-1}. Each copolymer (10 mg) was dried for at least 24 h in a vacuum oven at 70 °C prior to analysis. Dried samples were hermetically sealed in a vented aluminium pan, and the instrument was calibrated for heat flow and temperature using both indium and zinc standards. Samples were annealed at 100 °C for 5 min before cooling to −90 °C and maintaining this temperature for 1 min. The T_g was then determined by heating the copolymer up to 100 °C and taken as a midpoint value.

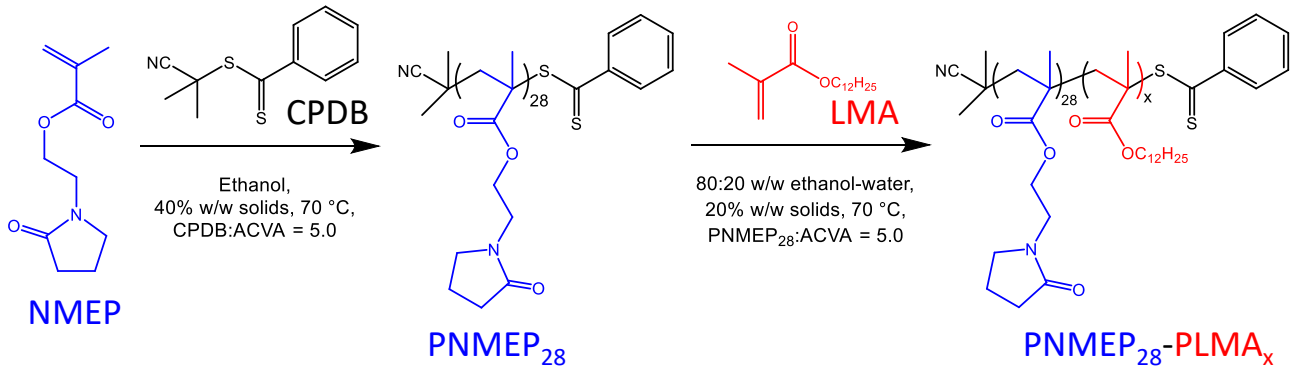

Scheme 1 Synthesis of a $PNMEP_{28}$ macro-CTA by RAFT solution polymerization of NMEP in ethanol at 70 °C and subsequent synthesis of $PNMEP_{28}$-$PLMA_x$ diblock copolymer nano-objects in an 80:20 w/w ethanol-water mixture by RAFT dispersion polymerization of LMA at 70 °C.

Results and discussion

A $PNMEP_{28}$ macro-CTA was prepared by RAFT solution polymerisation of NMEP in ethanol at 70 °C using a CPDB RAFT agent, see Scheme 1. This polymerisation was allowed to progress for 270 min and was quenched at 90% conversion. The mean DP was determined to be 28 by end-group analysis using ^{1}H NMR spectroscopy.

This $PNMEP_{28}$ macro-CTA was subsequently chain-extended via RAFT dispersion polymerisation of LMA at 20% w/w solids in an 80:20 w/w ethanol-water mixture at 70°C. The aqueous solubility of LMA is too low for an aqueous emulsion polymerisation formulation[38] while it is difficult to achieve high monomer conversions in pure ethanol owing to the relatively slow polymerisation kinetics under such conditions.[25,39] Thus, an 80:20 w/w ethanol-water mixture was selected for the RAFT dispersion polymerisation of LMA. This formulation enabled very high LMA conversions to be achieved within 11 h at 70 °C. A series of $PNMEP_{28}$-$PLMA_x$ diblock copolymer nano-objects were synthesised by targeting PLMA/PNMEP mass ratios ranging from 2:1 to 7:1 at 80:20 w/w ethanol-water mixtures (Figure 1). Both high and low molecular weight shoulders are observed in the GPC curves obtained for all target diblock copolymers. Utilising UV GPC (Figure 1b), whereby the detector wavelength is tuned to the absorption of the dithiobenzoate chain-ends (308 nm), it is clear that the polymer chains in both these minor populations retain their RAFT end-groups. This suggests that the low molecular weight shoulder is simply the result of slow/incomplete reinitiation of the $PNMEP_{28}$ precursor, rather than premature loss of RAFT end-groups. We attribute the high molecular weight shoulder to chain transfer to polymer, rather than dimethacrylate impurities in the LMA monomer. High LMA conversions (>98%) were achieved in all cases as shown by ^{1}H NMR spectroscopy. However, this technique becomes rather insensitive for low corations of residual monomer (< 1%). For potential industrial applications, the level of volatile organic compounds (VOCs) in such formulations are very important. Thus, gas chromatography (GC) analysis was used to quantify the level of unreacted LMA monomer while reverse-phase high performance liquid chromatography (HPLC) was utilised to determine residual NMEP monomer. GC analysis indicated LMA contents of less than 0.15% (1500 ppm) while HPLC indicated that less than 0.03% NMEP (300 ppm) remained in the original copolymer dispersions. For the two shortest diblock copolymers, GC

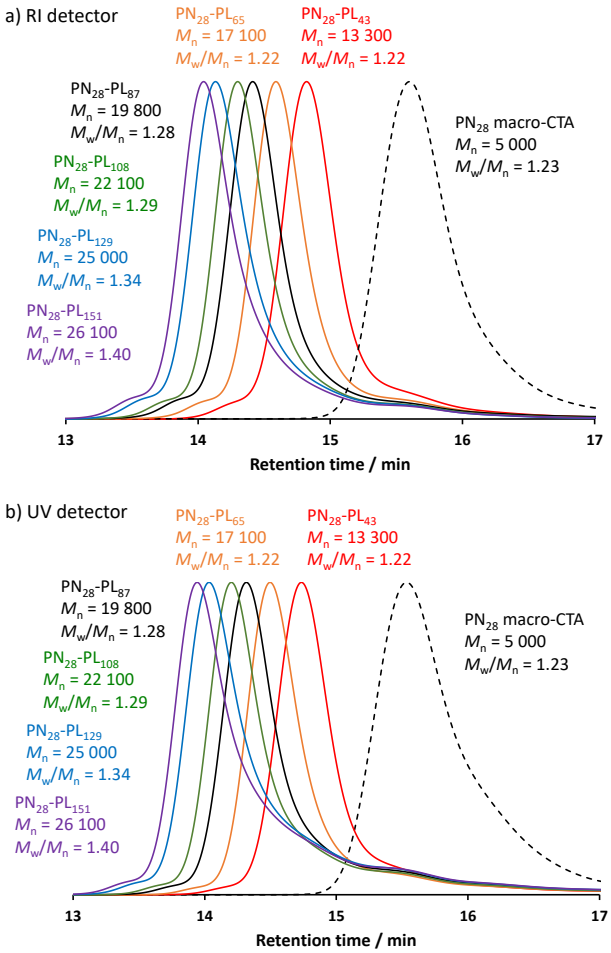

Figure 1. Chloroform GPC curves recorded for a series of $PNMEP_{28}$-$PLMA_x$ diblock copolymers and the corresponding $PNMEP_{28}$ precursor: (a) refractive index detector with calibration using a series of near-monodisperse poly(methyl methacrylate) standards; (b) UV detection at λ = 308 nm.

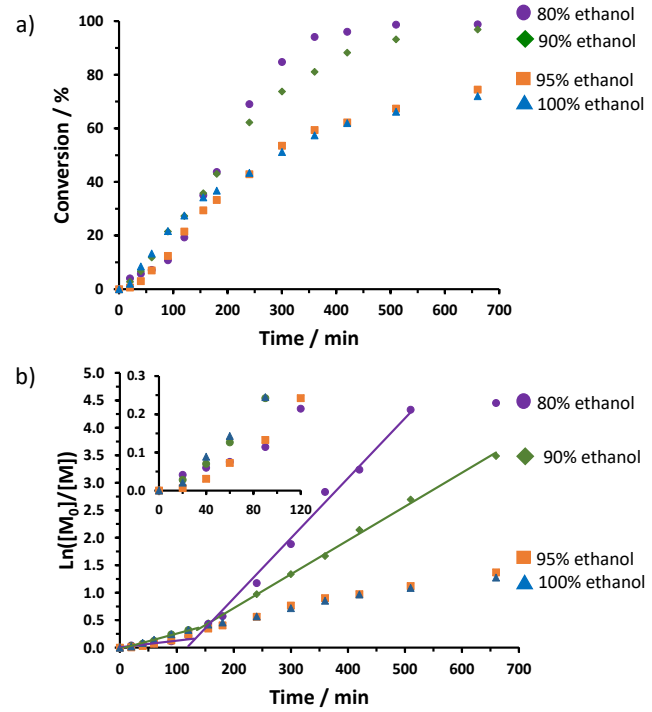

Figure 2.(a) Conversion vs. time curves obtained for the RAFT dispersion polymerisation of LMA at 70 °C using a $PNMEP_{28}$ macro-CTA and ACVA initiator ([PNMEP]/[ACVA] = 5.0) at 20% w/w solids. LMA conversions were determined by ^{1}H NMR spectroscopy. In each case, a $PNMEP_{28}$-$PLMA_{87}$ composition was targeted and the solvent composition was varied from absolute ethanol to an 80:20 w/w ethanol-water mixture. (b) The same data presented as semi-logarithmic plots, the data points obtained for the first two hours are magnified in the inset.

analysis was not conducted owing to poor partitioning of these low molecular weight chains with the solvent.

The polymerisation kinetics were monitored for various ethanol-water mixtures (containing 0, 5, 10 or 20% water by mass) targeting a $PNMEP_{28}$-$PLMA_{87}$ diblock composition. It is clear that increasing the proportion of water as a co-solvent significantly increases the rate of LMA polymerisation, as previously reported by other workers.[21,25] For example, using an

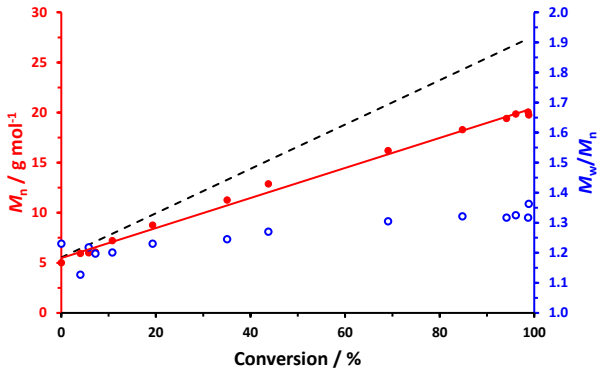

Figure 3. Evolution of M_n (●) and M_w/M_n (○) with conversion obtained during the RAFT dispersion polymerisation of LMA at 70 °C targeting $PNMEP_{28}$-$PLMA_{87}$ in 80:20 w/w ethanol-water at 20% w/w solids concentration. The theoretical M_n is indicated by the black dashed line.

80:20 w/w ethanol-water mixture enabled 99% LMA conversion to be achieved within 8.5 h. Hence this solvent composition was utilised for all of the PISA syntheses reported in this study.

The corresponding semi-logarithmic plots (Figure 2b) indicate markedly faster polymerisations after nucleation as the proportion of water was increased. Prior to micellar nucleation, there appears to be no trend in the polymerisation rates observed as the water content is systematically increased (see inset in Figure 2b). We currently have no satisfactory explanation for these observations. However, a noticeable rate enhancement occurred at approximately the same LMA conversion for the 90:10 and 80:20 w/w solvent compositions, suggesting that a critical PLMA DP of 17 is required for nucleation. This is significantly lower than that reported by Jones and co-workers, who estimated a critical DP of 50 for PBzMA chains grown from a PDMA precursor in the same conditions.[25] The rate enhancement was significantly higher for 20% w/w water compared to 10% w/w water, with the latter formulation only reaching an LMA conversion of 93% within the same 8.5 h time period. Using 20% w/w water, a relatively high conversion (~99%) was achieved within 8.5 h.

Table 1 Summary of the target diblock copolymer compositions, LMA monomer conversions, residual levels of NMEP and LMA monomer, molecular weight data and glass transition temperature (T_g) values.

Target diblock copolymer composition	LMA conversion[a] / %	Residual NMEP[b] / ppm	Residual LMA[c] / ppm	M_n[d] / g mol^{-1}	M_w/M_n[d]	PLMA T_g[e] / °C	PNMEP T_g / °C
$PNMEP_{28}$ macro-CTA	N/A	n.d.	N/A	5 000	1.23	N/A	65
$PNMEP_{28}$-$PLMA_{43}$	>99	136	n.d.	13 300	1.22	-48	56
$PNMEP_{28}$-$PLMA_{65}$	>99	309	n.d.	17 100	1.22	-48	56
$PNMEP_{28}$-$PLMA_{87}$	>99	199	983	19 800	1.28	-46	52
$PNMEP_{28}$-$PLMA_{108}$	99	132	1037	22 100	1.29	-47	49
$PNMEP_{28}$-$PLMA_{129}$	99	155	1156	25 000	1.34	-48	49
$PNMEP_{28}$-$PLMA_{151}$	99	168	1153	26 100	1.40	-47	50

[a] LMA conversion determined by ^{1}H NMR spectroscopy. [b] Determined by HPLC- [c] Determined by gas chromatography [d] Determined by chloroform GPC. [e] Determined by DSC. [N.B. 'n.d.' is shorthand for 'not determined'].

However to ensure maximum conversion for all target diblock copolymers, each polymerisation was allowed to proceed overnight (16 h). The same diblock composition was also targeted using anhydrous ethanol. The conversion vs. time curve and semi-logarithmic plot was almost identical to that observed using either 5% w/w water or laboratory-grade ethanol (see Figure 2 and Figure S3), suggesting that such low levels of water has a negligible effect on the polymerisation kinetics. The final LMA conversion obtained after 11 h at 70 °C for the laboratory-grade ethanol (designated 100% ethanol) was 72%, whereas 68% conversion was achieved for the anhydrous ethanol formulation under the same conditions. The molecular weight and dispersity were plotted against conversion for the kinetics conducted using an 80:20 w/w ethanol-water mixture (Figure 3). The linear evolution in M_n with increasing conversion indicates good RAFT control. The observed deviation from the theoretical M_n at high conversions was not unexpected because molecular weights were calculated against a PMMA calibration.

The glass transition temperature (T_g) associated with each $PNMEP_{28}$-$PLMA_x$ diblock copolymer was determined by DSC after annealing at 100°C to remove traces of solvent (Figure S4). In all cases, these copolymers are distinctly PLMA-rich, which means that the T_g for the PNMEP cannot be easily detected. The T_g of the $PNMEP_{28}$ macro-CTA was 65 °C. For the diblock copolymers, the $PLMA_x$ T_g was fairly constant around -48 °C, which is somewhat higher than the reported literature value of –65 °C.[32] Similarly, for the diblock copolymer series the T_g of the $PNMEP_{28}$ block was suppressed by 10 - 15 °C for PLMA DPs above 87. The target diblock compositions are highly asymmetric in favour of PLMA, hence this block should be more easily detectable. This change in T_g for the PLMA and PNMEP blocks respectively indicated some degree of miscibility between the two blocks. In this context, a study of diblock copolymers comprising tert-butyldimethylsilyl methacrylate (TBDMSiMA) and poly(dimethylsiloxane) methacrylate (PDMSMA) by Lejars *et al.* is noteworthy[40] These workers observed that the T_g of the PTBDMSiMA block (82 °C) was somewhat lower than that of the corresponding PTBDMSiMA homopolymer (105 °C), whereas the T_g for the PDMSMA block was higher than that of the corresponding homopolymer (-114 °C *vs* -123 °C). Moreover, greater microphase separation was observed for longer PDMSMA blocks so the T_g values for the individual blocks were closer to those for the corresponding homopolymers. It was concluded that the PDMSMA chains had a plasticising effect on the PTBDMSiMA block, which led to partially miscible behaviour and hence only weak segregation. This behaviour is also observed for the $PNMEP_{28}$-$PLMA_x$ diblock copolymers as the T_g of the $PLMA_x$ and $PNMEP_{28}$ block are increased and decreased respectively with regard to their homopolymers.

Despite the relatively low *T*g values for the insoluble PLMA block, these diblock copolymer nano-objects could be imaged by transmission electron microscopy (TEM). For all targeted copolymer compositions, the predominant morphology appeared to be spheres (see Figure 4). However, minor populations of lamellar sheets were also observed in all cases. In many instances PISA syntheses only produce kinetically-trapped spheres.[15,25,41,42] This is particularly true in the case of RAFT emulsion polymerisation,[42–49] but it is also well-known for RAFT dispersion polymerisation when using a relatively long steric stabiliser block[31,50–52] or when working at relatively low copolymer concentration.[50,53] However, so-called higher order morphologies such as worms, vesicles or lamellae can be obtained under appropriate conditions. [50,54–58] Typically, this involves using a suitable short steric stabiliser block and targeting a relatively long insoluble block at a sufficiently high

Table 2 Summary of TEM and SAXS data obtained for $PNMEP_{28}$-$PLMA_x$ diblock copolymer nanoparticles.

Target diblock composition	TEM[a]	SAXS[b]			
	Number-average diameter / nm	Volume-average diameter / nm	R_g / nm	Membrane thickness / nm	N_{agg}
$PNMEP_{28}$-$PLMA_{43}$	66 ± 23	N/A	N/A	N/A	N/A
$PNMEP_{28}$-$PLMA_{65}$	155 ± 58	174 ± 61	2.5	13.4 ± 1.1	32 500
$PNMEP_{28}$-$PLMA_{87}$	181 ± 40	166 ± 48	2.2	16.5 ± 2.1	26 200
$PNMEP_{28}$-$PLMA_{108}$	207 ± 77	161 ± 38	2.1	18.8 ± 2.3	21 500
$PNMEP_{28}$-$PLMA_{129}$	200 ± 49	153 ± 25	2.6	22.7 ± 3.3	17 600
$PNMEP_{28}$-$PLMA_{151}$	212 ± 64	150 ± 28	2.1	25.1 ± 4.4	15 700

[a] At least 100 particles were analysed per sample. [b] SAXS measurements were performed on 1.0% w/w copolymer dispersions diluted using an 80:20 w/w ethanol-water mixture. R_g is the radius of gyration of the coronal stabiliser (PNMEP) chains and N_{agg} is the mean vesicle aggregation number.

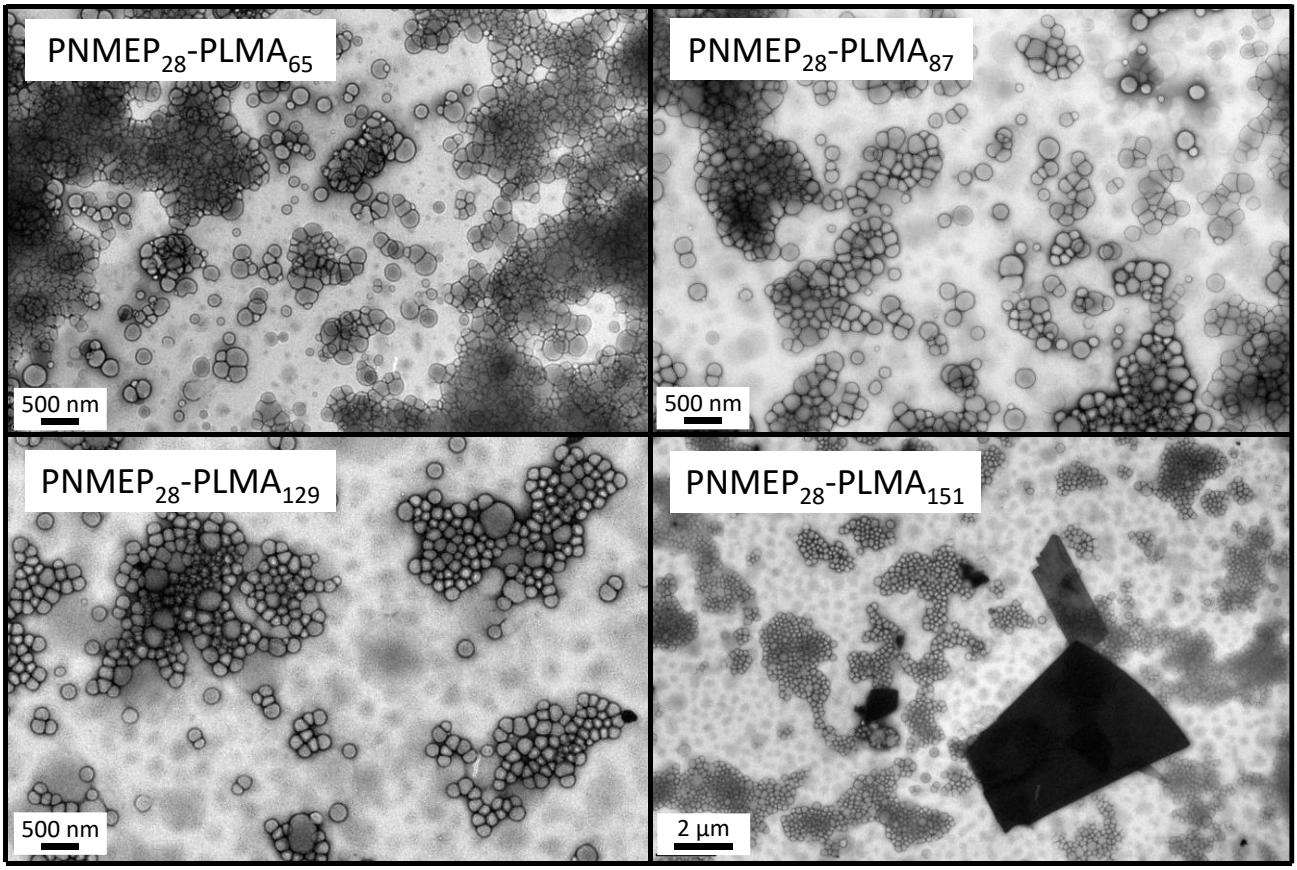

Figure 4. Representative TEM images recorded for dried dilute aqueous dispersions of $PNMEP_{28}$-$PLMA_x$ diblock copolymer nano-objects prepared via RAFT dispersion polymerisation of LMA in an 80:20 w/w ethanol-water mixture. A spherical morphology is observed in all cases with a minor population of lamellar sheets present in some samples. A lower magnification image is shown for $PNMEP_{28}$-$PLMA_{152}$ (note 2 µm scale bar) to more clearly show the relatively large lamellar sheets that are present in this dispersion. Subsequent SAXS studies indicated that some of the 'spheres' are actually vesicles (see Figures S6 and S7 in ESI).

copolymer concentration.[56,59–61] For such PISA formulations, the evolution in copolymer morphology always seems to follow the same mechanistic pathway. Spheres are formed initially and, as the structure-directing insoluble block grows longer, worms are formed via the stochastic 1D fusion of multiple spheres, followed by vesicle formation via transient jellyfish-like intermediates if a sufficiently asymmetric diblock copolymer composition is targeted.[57,62,63] Under certain conditions, block copolymer lamellae (i.e. thin sheets or platelets) can also be formed.[64,65]

In view of this literature precedent, it seemed rather surprising that spheres would co-exist with lamellae. Thus small angle X-ray scattering (SAXS) was used to examine these diblock copolymer morphologies in more detail. Satisfactory data fits could be obtained using a vesicle model (see Figure 5) for five of the six entries shown in Table 2. Moreover, the low *q* gradient was close to -2, which is consistent with the formation of vesicles (and lamellae).[66] Inspecting the first entry in Table 1 ($PNMEP_{28}$-$PLMA_{43}$), TEM studies initially suggested a broad size distribution of spheres (see Inset of Figure S6) but the corresponding SAXS pattern could not be fitted to a spherical model (see Figure S7). Instead, this SAXS pattern was fitted using a two-population vesicle plus sphere model to obtain a mean sphere diameter of 32 nm and a vesicle diameter of 76 nm with an associated membrane thickness of 10.0 nm (Figure S6). TEM studies indicate an apparent increase in mean vesicle diameter when targeting higher DPs for the membrane-forming PLMA block. However, given the low T_g of the PLMA block these vesicles are expected to be rather deformable – indeed there is no direct evidence for membranes in the TEM images. Moreover, the number-average vesicle diameters estimated by TEM exceed the volume-average diameters determined by SAXS. This is physically unrealistic, which again suggests significant deformation (flattening) of the original vesicle morphology during drying. Moreover, when calculating mean TEM diameters we only analysed 100 vesicles per copolymer. Thus the TEM data are far less statistically robust than that obtained by SAXS, for which the X-ray scattering is averaged over many millions of vesicles. SAXS studies indicated a modest reduction in the mean vesicle diameter from 174 nm to 150 nm on increasing the PLMA DP (see entries 2-6 in Table 2). This is accompanied by a significant reduction in the vesicle polydispersity. Moreover, thicker vesicle membranes (from 13.4 nm to 25.1 nm) are obtained on increasing the PLMA DP,

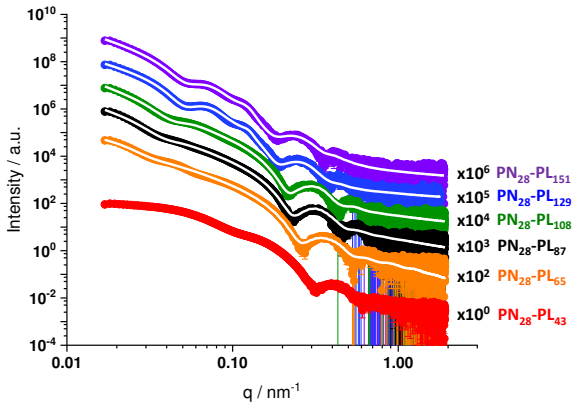

Figure 5. SAXS patterns recorded for 1.0% w/w copolymer dispersions in 80:20 w/w ethanol-water at 20 °C: $PNMEP_{28}$-$PLMA_{43}$ (red), $PNMEP_{28}$-$PLMA_{65}$ (orange), $PNMEP_{28}$-$PLMA_{87}$ (black), $PNMEP_{28}$-$PLMA_{108}$ (green), $PNMEP_{28}$-$PLMA_{129}$ (blue) and $PNMEP_{28}$-$PLMA_{151}$ (purple). The white lines indicate data fits obtained using a well-known vesicle model for five of the patterns.[96] See figure.. in SI… for the $PNMEP_{28}$-$PLMA_{43}$ fit. Each SAXS pattern is offset by an arbitrary factor for clarity.

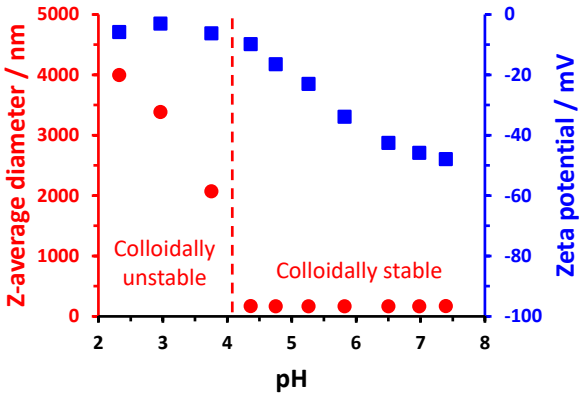

Figure 6. Zeta potential (■) and z-average diameter (●) vs. solution pH curves obtained for $PNMEP_{28}$-$PLMA_{87}$ nanoparticles prepared using a carboxylic acid-functionalised initiator (ACVA) for both blocks. At pH 7, the z-average diameter is 168 nm and the zeta potential is -46 mV.

while there is a systematic reduction in the mean aggregation number (N_{agg}) from 32 500 to 15 700. Interestingly, a structure peak is observed in the scattering patterns for the two most PLMA-rich diblock copolymer compositions (entries 5 and 6 in Table 2). This feature is tentatively assigned to lamellar stacking and suggests a mean inter-lamellar spacing of 51 and 53 nm for the PLMA DP of 129 and 151 respectively. To account for this lamella stacking, a Gaussian peak was added to the vesicle fit at 0.1 nm^{-1}.[67] One reviewer has suggested that this SAXS feature could indicate the presence of multilamellar vesicles. TEM analysis provides no evidence for such nano-objects but we are unable to categorically rule out this possibility.

The highly asymmetric nature of these diblock copolymers coupled with the weakly hydrophilic nature of the PNMEP stabiliser block[14] suggests that they should not be colloidally stable in water. Recently, we reported that PNMEP could be used as an electrosteric stabiliser block for aqueous PISA syntheses.[15] However, colloidal stability was only conferred if the terminal carboxylic acid end-group on the PNMEP chain was in its ionised anionic form – macroscopic precipitation was always observed if the aqueous solution pH was lower than pH 7. This is an example of so-called electrosteric stabilisation. In view of these prior observations, we did not expect the $PNMEP_{28}$-$PLMA_x$ nano-objects prepared in the present study to remain stable when diluted from their original 80:20 w/w ethanol-water mixture using deionised water. This is because the CPDB RAFT agent used for such PISA syntheses does not confer any ionic end-groups to supplement the rather weak steric stabilisation provided by the non-ionic PNMEP chains. However, preliminary DLS experiments indicated that the colloidal stability of such nanoparticles was retained in dilute aqueous solution (Figure S8). Remarkably, no aggregation was observed even when heating up to 90 °C, despite the well-documented inverse temperature-solubility behaviour observed for PNMEP.[14,15] To better understand these unexpected observations, zeta potential measurements were undertaken. Given the non-ionic nature of the CPDB RAFT agent, so the nanoparticle zeta potential was expected to be close to zero. Instead, a zeta potential of -46 mV was obtained at pH 7. However, it is well known that a minor proportion of RAFT-synthesised polymer chains can be capped by end-groups originating from the initiator.[68] Thus, this negative surface charge is conferred by the carboxylic acid-based azo initiator (ACVA) used in the macro-CTA synthesis and this is sufficient to confer electrostatic stabilisation on the nanoparticles in water. Moreover, the sharp upturn in apparent particle size observed at lower pH occurs below pH 4.3. Given that the pK_a for carboxylic acid-capped non-ionic water-soluble polymer chains lies between 4.67[69] and 5.10,[15] this suggests that colloidal instability only occurs when most of the $PNMEP_{28}$ stabiliser chain-ends become protonated (see Figure 6).

In summary, the RAFT synthesis of $PNMEP_{28}$ macro-CTA using CPDB combined with ACVA results in a significant proportion of carboxylic acid-terminated stabiliser chains, which is sufficient to account for the unexpected colloidal stability observed for the corresponding $PNMEP_{28}$-$PLMA_x$ vesicles in dilute aqueous solution.

RAFT end-group removal from PNMEP-PLMA diblock copolymer nano-objects using visible light irradiation

One well-known disadvantage of RAFT polymerisation is that the sulfur-based chain transfer agent confers both colour and malodour on the final copolymer.[17,70] In view of this, considerable effort has been devoted to the post-polymerisation removal of RAFT end-groups.[71,72] Most of these studies have involved either thermolysis or the use of selective reagents to cleave the organosulfur groups from the chain-ends.[73–76] Moreover, the vast majority of work in this area has focused on the modification of soluble chains,[77–85] with only a few studies examining RAFT end-group removal from block copolymer nano-objects.[86,87]

Mattson and co-workers used UV light (λ = 380nm) to remove terminal trithiocarbonate end-groups with a photoredox

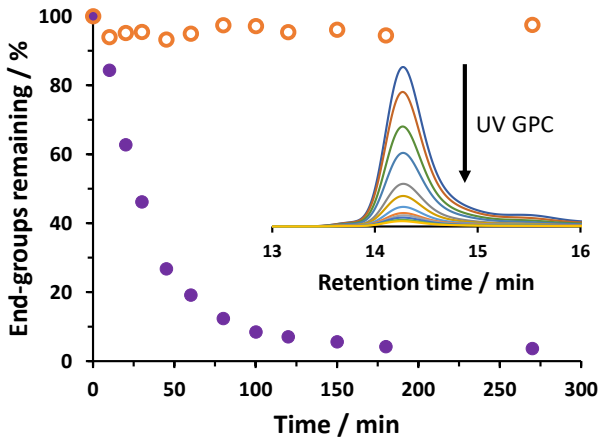

Figure 7. Relative reduction in dithiobenzoate end-group concentration over time for a 7.5% w/w aqueous dispersion of $PNMEP_{28}$-$PLMA_{87}$ vesicles after continuous irradiation for 4.5 h using blue LED light (λ = 405 nm, 0.37 mW cm^{-2}) at 50 °C (●) and the corresponding data when using 5 molar equivalents of H_2O_2 to end-group at the same temperature (○). Inset shows the reduction in UV GPC signal over time during the LED experiment.

catalyst in solution (acetonitrile or *N,N*-dimethylacetamide).[83] This method was shown to be compatible with many monomer classes and did not require elevated temperatures or deoxygenation. Discekici *et al.* were the first to report using visible light (λ = 465 nm) to remove trithiocarbonate end-groups from polystyrene chains dissolved in dichloromethane.[88] They found that using both an auxiliary amine and visible light was essential to produce a hydrogen chain-end; in the absence of light irridation, aminolysis produced thiol end-groups.

Matioszek and co-workers used ozonolysis to remove xanthate-based RAFT end-groups buried within the cores of relatively low molecular weight poly(*n*-butyl acrylate) latex particles in aqueous media.[86] Complete removal of these RAFT end-groups was observed by UV GPC analysis within 1 h at room temperature. Colloidal stability was maintained provided that the M_n of the latex was above 5 000 g mol^{-1}. Recently, Jesson *et al.* utilised H_2O_2 to remove RAFT chain-ends from aqueous dispersions of diblock copolymer nano-objects.[87] In this case, 96% removal of dithiobenzoate end-groups from weakly hydrophobic poly(2-hydroxypropyl methacrylate) (PHPMA) cores was achieved within 8 h at 70 °C as judged by UV GPC analysis. However, this protocol required using excess H_2O_2 (H_2O_2/dithiobenzoate molar ratio = 5.0). Moreover, it was much more difficult to remove trithiocarbonate end-groups under the same conditions. Furthermore, removal of dithiobenzoate end-groups from PBzMA core-forming blocks proved to be problematic. Presumably, this is the result of restricted diffusion of the H_2O_2 reagent into such relatively hydrophobic nanoparticle cores. Both Matioszek and co-workers and Jesson et al. demonstrated that UV GPC was particularly useful for analysing the extent of removal of RAFT end-groups over time. This is because this technique ensures separation of the copolymer chains from any UV-absorbing low molecular weight products (e.g. benzoic acid) arising from chemical oxidation of the RAFT end-groups.

In view of this literature precedent, we examined the use of blue LED light (λ = 405 nm) to remove dithiobenzoate chain-ends from a 7.5 % w/w aqueous dispersion of $PNMEP_{28}$-$PLMA_{87}$ diblock copolymer vesicles. This protocol was adopted because our preliminary experiments suggested that it was difficult for various chemical reagents (e.g. ACVA, Luperox, H_2O_2 and benzylamine) to diffuse into the highly hydrophobic PLMA membranes (see Figure 7 for the failed attempt to remove end-groups using H_2O_2). As far as we are aware, there are no literature reports of using visible light to remove RAFT end-groups from diblock copolymer nano-objects. It should be noted that visible light can be used to control the polymerisation of methacrylates in the absence of initiators by generating radicals by excitation of the spin-forbidden $n \rightarrow \pi^*$ transition.[89–93]

An aqueous dispersion of $PNMEP_{28}$-$PLMA_{87}$ diblock copolymer nanoparticles was diluted to 7.5% w/w using deionised water and exposed to 405 nm light at 50 °C with continuous stirring. The rate of RAFT end-group removal was monitored for 4.5 h using UV GPC (Figure 7). UV GPC chromatograms were normalised with respect to the refractive index signal. After 60 min, 81% of the RAFT end-groups were removed. After 3 h, only 4% of the original RAFT end-groups remained. Unlike the H_2O_2 protocol reported by Jesson and co-workers, this visible light irradiation method requires a lower temperature, significantly shorter reaction times and no additional reagents to remove more than 95% dithiobenzoate end-groups from an aqueous dispersion of methacrylic diblock copolymer nano-objects. It is perhaps also worth emphasising that the water-insoluble PLMA blocks used in the present study are significantly more hydrophobic than the water-insoluble PHPMA and PBzMA blocks that comprised the cores of the nanoparticles reported by Jesson and coworkers.[87] In that prior study, ingress of the H_2O_2 reagent was relatively fast for the water-plasticised, weakly hydrophobic PHPMA cores but relatively slow for the more hydrophobic PBzMA cores. This reagent mass transport problem does not apply to the LED irradiation method, allowing rapid removal of dithiobenzoate end-groups even from highly hydrophobic PLMA cores. Given the growing interest in PISA syntheses using flow chemistry, visible light could prove to be useful for removing RAFT end-groups on a large scale.[94,95]

Conclusions

A $PNMEP_{28}$ macro-CTA was chain-extended with LMA in an 80:20 w/w ethanol-water mixture to produce a series of $PNMEP_{28}$-$PLMA_x$ diblock copolymer nano-objects. Despite the well-documented low T_g for the insoluble PLMA block, good-quality TEM images could be obtained for this PISA formulation. For x = 43, a mixed sphere and vesicle morphology was observed, while polydisperse vesicles were obtained for x values ranging between 65 and 151. However, no worm phase could be identified. SAXS studies confirmed the copolymer morphologies assigned by TEM. Slightly smaller vesicles with lower mean aggregation numbers and thicker membranes were obtained when targeting higher PLMA DPs. A minor population of sheet-like lamellae was observed for each target copolymer composition, with lamellar stacking leading to a structure peak

in the scattering patterns recorded for $PNMEP_{28}$-$PLMA_{129}$ and $PNMEP_{28}$-$PLMA_{151}$. Unexpectedly, these $PNMEP_{28}$-$PLMA_x$ nanoparticles proved to be colloidally stable when diluted with deionised water to afford dilute aqueous dispersions. Zeta potential studies indicate that such colloidal stability is conferred by initiator-derived carboxylic acid end-groups located on some of the non-ionic PNMEP stabiliser chains. Finally, 96% of dithiobenzoate chain-ends could be removed within 3 h at 50 °C via LED irradiation of a 7.5% aqueous dispersion of $PNMEP_{28}$-$PLMA_{87}$ vesicles at a wavelength of 405 nm. This appears to be an attractive method for RAFT chain-end removal from diblock copolymer nano-objects, particularly for those with highly hydrophobic cores for which ingress of chemical reagents such as H_2O_2 is relatively slow.

Conflicts of interest

There are no conflicts to declare.

Acknowledgements

Alastair Veitch is thanked for obtaining the residual monomer concentrations by LC and GC. EPSRC is thanked for funding a CDT PhD studentship for the first author (EP/L016281). Ashland Specialty Ingredients (Bridgewater, New Jersey, USA) is thanked for partial financial support of this PhD project, for supplying the NMEP monomer and for permission to publish this work. SPA also thanks the ERC for a five-year Advanced Investigator grant (PISA 320372) and the EPSRC for an Established Career Particle Technology Fellowship (EP/R003009).

References

1 M. Teodorescu and M. Bercea, *Polym. Plast. Technol. Eng.*, 2015, **54**, 923–943.
2 X. Sun, Z. Cao, C. K. Yeh and Y. Sun, *Colloids Surfaces B Biointerfaces*, 2013, **110**, 96–104.
3 F. Haaf, A. Sanner and F. Straub, *Polym. J.*, 1985, **17**, 143–152.
4 N. Bailly, M. Thomas and B. Klumperman, *Biomacromolecules*, 2012, **13**, 4109–4117.
5 A. J. Hoteling, W. F. Nichols, P. S. Harmon, S. M. Conlon, I. M. Nuñez, J. W. Hoff, O. M. Cabarcos, R. B. Steffen and D. J. Hook, *J. Biomed. Mater. Res. Part B Appl. Biomater.*, 2018, **106**, 1064–1072.
6 H. U. Kang, Y. C. Yu, S. J. Shin, J. Kim and J. H. Youk, *Macromolecules*, 2013, **46**, 1291–1295.
7 G. Pound, F. Aguesse, J. B. McLeary, R. F. M. Lange and B. Klumperman, *Macromolecules*, 2007, **40**, 8861–8871.
8 T. L. U. Nguyen, K. Eagles, T. P. Davis, C. Barner-Kowollik and M. H. Stenzel, *J. Polym. Sci. Part A Polym. Chem.*, 2006, **44**, 4372–4383.
9 N. Fandrich, J. Falkenhagen, S. M. Weidner, D. Pfeifer, B. Staal, A. F. Thünemann and A. Laschewsky, *Macromol. Chem. Phys.*, 2010, **211**, 869–878.
10 J. Deng, Y. Shi, W. Jiang, Y. Peng, L. Lu and Y. Cai, *Macromolecules*, 2008, **41**, 3007–3014.
11 J. Zhang, M. Zou, J. Dong and X. Li, *Colloid Polym. Sci.*, 2013, **291**, 2653–2662.
12 V. J. Cunningham, Y. Ning, S. P. Armes and O. M. Musa, *Polymer.*, 2016, **106**, 189–199.
13 V. J. Cunningham, S. P. Armes and O. M. Musa, *Polym. Chem.*, 2016, **7**, 1882–1891.
14 V. J. Cunningham, M. J. Derry, L. A. Fielding, O. M. Musa and S. P. Armes, *Macromolecules*, 2016, **49**, 4520–4533.
15 R. R. Gibson, S. P. Armes, O. M. Musa and A. Fernyhough, *Polym. Chem.*, 2019, **10**, 1312–1323.
16 N. J. Warren, O. O. Mykhaylyk, D. Mahmood, A. J. Ryan and S. P. Armes, *J. Am. Chem. Soc.*, 2014, **136**, 1023–1033.
17 S. L. Canning, G. N. Smith and S. P. Armes, *Macromolecules*, 2016, **49**, 1985–2001.
18 B. Charleux, G. Delaittre, J. Rieger and F. D'Agosto, *Macromolecules*, 2012, **45**, 6753–6765.
19 J. Zhou, H. Yao and J. Ma, *Polym. Chem.*, 2018, 9, 2532–2561.
20 F. D'Agosto, J. Rieger and M. Lansalot, *Angew. Chemie Int. Ed.*, , DOI:10.1002/anie.201911758.
21 X. Zhang, J. Rieger and B. Charleux, *Polym. Chem.*, 2012, **3**, 1502.
22 Y. Su, X. Xiao, S. Li, M. Dan, X. Wang and W. Zhang, *Polym. Chem.*, 2014, **5**, 578–587.
23 C. Gao, S. Li, Q. Li, P. Shi, S. A. Shah and W. Zhang, *Polym. Chem.*, 2014, **5**, 6957–6966.
24 C. Gao, J. Wu, H. Zhou, Y. Qu, B. Li and W. Zhang, *Macromolecules*, 2016, **49**, 4490–4500.
25 E. R. Jones, M. Semsarilar, P. Wyman, M. Boerakker and S. P. Armes, *Polym. Chem.*, 2016, **7**, 851–859.
26 S. M. North, E. R. Jones, G. N. Smith, O. O. Mykhaylyk, T. Annable and S. P. Armes, *Langmuir*, 2017, **33**, 1275–1284.
27 I. Van Nieuwenhove, S. Maji, M. Dash, S. Van Vlierberghe, R. Hoogenboom and P. Dubruel, *Polym. Chem.*, 2017, **8**, 2433–2437.
28 M. Tan, Y. Shi, Z. Fu and W. Yang, *Polym. Chem.*, 2018, **9**, 1082–1094.
29 H. Khan, M. Cao, W. Duan, T. Ying and W. Zhang, *Polymer.*, 2018, **150**, 204–213.
30 A. Rubio, G. Desnos and M. Semsarilar, *Macromol. Chem. Phys.*, 2018, **219**, 1800351.
31 L. A. Fielding, J. A. Lane, M. J. Derry, O. O. Mykhaylyk and S. P. Armes, *J. Am. Chem. Soc.*, 2014, **136**, 5790–5798.
32 S. Rogers and L. Mandelkern, *J. Phys. Chem.*, 1957, **61**, 985–991.
33 R. Y. Lochhead, in *Cosmetic Nanotechnology*, American Chemical Society, 2007, vol. 961, pp. 3–56.
34 F. Zeng and L. Zhang, *Water resistant personal care polymers, US9486399B2*, 2016.
35 X. He, B. Wang, X. Li and J. Dong, *RSC Adv.*, 2019, **9**, 28102–28111.
36 X. He, X. Li and J. Dong, *Colloids Surfaces A Physicochem. Eng. Asp.*, 2019, **577**, 493–499.
37 Y. Pei, N. C. Dharsana, J. A. Van Hensbergen, R. P. Burford, P. J. Roth and A. B. Lowe, *Soft Matter*, 2014, **10**, 5787–5796.
38 K. Tauer, A. M. I. Ali, U. Yildiz and M. Sedlak, *Polymer.*, 2005, **46**, 1003–1015.
39 Y. Pei and A. B. Lowe, *Polym. Chem.*, 2014, **5**, 2342–2351.
40 M. Lejars, A. Margaillan and C. Bressy, *Polym. Chem.*, 2013, **4**, 3282.
41 J. Rieger, F. Stoffelbach, C. Bui, D. Alaimo, C. Jérôme and B. Charleux, *Macromolecules*, 2008, **41**, 4065–4068.
42 J. Rieger, W. Zhang, F. Stoffelbach and B. Charleux, *Macromolecules*, 2010, **43**, 6302–6310.
43 C. J. Ferguson, R. J. Hughes, D. Nguyen, B. T. T. Pham, R. G. Gilbert, A. K. Serelis, C. H. Such and B. S. Hawkett, *Macromolecules*, 2005, **38**, 2191–2204.
44 I. Chaduc, A. Crepet, O. Boyron, B. Charleux, F. D'Agosto and M. Lansalot, *Macromolecules*, 2013, **46**, 6013–6023.
45 V. J. Cunningham, A. M. Alswieleh, K. L. Thompson, M. Williams, G. J. Leggett, S. P. Armes and O. M. Musa, *Macromolecules*, 2014, **47**, 5613–5623.

46 N. P. Truong, M. V. Dussert, M. R. Whittaker, J. F. Quinn and T. P. Davis, *Polym. Chem.*, 2015, **6**, 3865–3874.
47 B. Akpinar, L. A. Fielding, V. J. Cunningham, Y. Ning, O. O. Mykhaylyk, P. W. Fowler and S. P. Armes, *Macromolecules*, 2016, **49**, 5160–5171.
48 A. A. Cockram, R. D. Bradley, S. A. Lynch, P. C. D. Fleming, N. S. J. Williams, M. W. Murray, S. N. Emmett and S. P. Armes, *React. Chem. Eng.*, 2018, **3**, 645–657.
49 C. P. Jesson, V. J. Cunningham, M. J. Smallridge and S. P. Armes, *Macromolecules*, 2018, **51**, 3221–3232.
50 A. Blanazs, A. J. Ryan and S. P. Armes, *Macromolecules*, 2012, **45**, 5099–5107.
51 M. J. Derry, L. A. Fielding, N. J. Warren, C. J. Mable, A. J. Smith, O. O. Mykhaylyk and S. P. Armes, *Chem. Sci.*, 2016, **7**, 5078–5090.
52 E. R. Jones, O. O. Mykhaylyk, M. Semsarilar, M. Boerakker, P. Wyman and S. P. Armes, *Macromolecules*, 2016, **49**, 172–181.
53 A. P. Lopez-Oliva, N. J. Warren, A. Rajkumar, O. O. Mykhaylyk, M. J. Derry, K. E. B. Doncom, M. J. Rymaruk and S. P. Armes, *Macromolecules*, 2015, **48**, 3547–3555.
54 W. D. He, X. L. Sun, W. M. Wan and C. Y. Pan, *Macromolecules*, 2011, **44**, 3358–3365.
55 W. M. Wan, X. L. Sun and C. Y. Pan, *Macromolecules*, 2009, **42**, 4950–4952.
56 S. Boissé, J. Rieger, K. Belal, A. Di-Cicco, P. Beaunier, M. H. Li and B. Charleux, *Chem. Commun.*, 2010, **46**, 1950–1952.
57 D. Zehm, L. P. D. Ratcliffe and S. P. Armes, *Macromolecules*, 2013, **46**, 128–139.
58 P. Yang, L. P. D. Ratcliffe and S. P. Armes, *Macromolecules*, 2013, **46**, 8545–8556.
59 X. Zhang, S. Boissé, W. Zhang, P. Beaunier, F. D'Agosto, J. Rieger and B. Charleux, *Macromolecules*, 2011, **44**, 4149–4158.
60 S. Boissé, J. Rieger, G. Pembouong, P. Beaunier and B. Charleux, *J. Polym. Sci. Part A Polym. Chem.*, 2011, **49**, 3346–3354.
61 W. Zhang, F. D'Agosto, O. Boyron, J. Rieger and B. Charleux, *Macromolecules*, 2012, **45**, 4075–4084.
62 A. Blanazs, J. Madsen, G. Battaglia, A. J. Ryan and S. P. Armes, *J. Am. Chem. Soc.*, 2011, **133**, 16581–16587.
63 M. J. Derry, L. A. Fielding and S. P. Armes, *Prog. Polym. Sci.*, 2016, **52**, 1–18.
64 P. Yang, L. P. D. Ratcliffe and S. P. Armes, *Macromolecules*, 2013, **46**, 8545–8556.
65 P. Yang, O. O. Mykhaylyk, E. R. Jones and S. P. Armes, *Macromolecules*, 2016, **49**, 6731–6742.
66 O. Glatter and O. Kratky, *Small angle X-ray scattering*, Academic Press, New York, 1982.
67 M. J. Derry, O. O. Mykhaylyk, A. J. Ryan and S. P. Armes, *Chem. Sci.*, 2018, **9**, 4071–4082.
68 G. Moad, E. Rizzardo and S. H. Thang, *Acc. Chem. Res.*, 2008, **41**, 1133–1142.
69 J. R. Lovett, N. J. Warren, L. P. D. Ratcliffe, M. K. Kocik and S. P. Armes, *Angew. Chemie Int. Ed.*, 2015, **54**, 1279–1283.
70 S. Perrier, *Macromolecules*, 2017, **50**, 7433–7447.
71 Y. K. Chong, G. Moad, E. Rizzardo and S. H. Thang, *Macromolecules*, 2007, **40**, 4446–4455.
72 H. Willcock and R. K. O'Reilly, *Polym. Chem.*, 2010, **1**, 149–157.
73 B. Chong, G. Moad, E. Rizzardo, M. Skidmore and S. H. Thang, *Aust. J. Chem.*, 2006, **59**, 755–762.
74 D. L. Patton, M. Mullings, T. Fulghum and R. C. Advincula, *Macromolecules*, 2005, **38**, 8597–8602.
75 R. N. Carmean, C. A. Figg, G. M. Scheutz, T. Kubo and B. S. Sumerlin, *ACS Macro Lett.*, 2017, **6**, 185–189.
76 E. J. Cornel, S. van Meurs, T. Smith, P. S. O'Hora and S. P. Armes, *J. Am. Chem. Soc.*, 2018, **140**, 12980–12988.
77 X. P. Qiu and F. M. Winnik, *Macromol. Rapid Commun.*, 2006, **27**, 1648–1653.
78 L. Nebhani, S. Sinnwell, A. J. Inglis, M. H. Stenzel, C. Barner-Kowollik and L. Barner, *Macromol. Rapid Commun.*, 2008, **29**, 1431–1437.
79 A. J. Inglis, M. H. Stenzel and C. Barner-Kowollik, *Macromol. Rapid Commun.*, 2009, **30**, 1792–1798.
80 C. Boyer and T. P. Davis, *Chem. Commun.*, 2009, 6029–6031.
81 C. Boyer, V. Bulmus and T. P. Davis, *Macromol. Rapid Commun.*, 2009, **30**, 493–497.
82 K. Zhou, H. Cao, P. Gao, Z. Cui, Y. Ding and Y. Cai, *Macromolecules*, 2016, **49**, 2189–2196.
83 K. M. Mattson, C. W. Pester, W. R. Gutekunst, A. T. Hsueh, E. H. Discekici, Y. Luo, B. V. K. J. Schmidt, A. J. McGrath, P. G. Clark and C. J. Hawker, *Macromolecules*, 2016, **49**, 8162–8166.
84 D. J. Lunn, E. H. Discekici, J. Read de Alaniz, W. R. Gutekunst and C. J. Hawker, *J. Polym. Sci. Part A Polym. Chem.*, 2017, **55**, 2903–2914.
85 P. Alagi, N. Hadjichristidis, Y. Gnanou and X. Feng, *ACS Macro Lett.*, 2019, **8**, 664–669.
86 D. Matioszek, P. E. Dufils, J. Vinas and M. Destarac, *Macromol. Rapid Commun.*, 2015, **36**, 1354–1361.
87 C. P. Jesson, C. M. Pearce, H. Simon, A. Werner, V. J. Cunningham, J. R. Lovett, M. J. Smallridge, N. J. Warren and S. P. Armes, *Macromolecules*, 2017, **50**, 182–191.
88 E. H. Discekici, S. L. Shankel, A. Anastasaki, B. Oschmann, I.-H. Lee, J. Niu, A. J. McGrath, P. G. Clark, D. S. Laitar, J. R. de Alaniz, C. J. Hawker and D. J. Lunn, *Chem. Commun.*, 2017, **53**, 1888–1891.
89 T. G. McKenzie, Q. Fu, E. H. H. Wong, D. E. Dunstan and G. G. Qiao, *Macromolecules*, 2015, **48**, 3864–3872.
90 K. Jung, C. Boyer and P. B. Zetterlund, *Polym. Chem.*, 2017, **8**, 3965–3970.
91 R. N. Carmean, T. E. Becker, M. B. Sims and B. S. Sumerlin, *CHEMPR*, 2017, **2**, 93–101.
92 J. R. Lamb, K. P. Qin and J. A. Johnson, *Polym. Chem.*, 2019, **10**, 1585–1590.
93 M. Rubens, P. Latsrisaeng and T. Junkers, *Polym. Chem.*, 2017, **8**, 6496–6505.
94 R. W. Lewis, R. A. Evans, N. Malic, K. Saito and N. R. Cameron, *Polym. Chem.*, 2018, **9**, 60–68.
95 N. Corrigan, L. Zhernakov, M. H. Hashim, J. Xu and C. Boyer, *React. Chem. Eng.*, 2019, **4**, 1216–1228.